LUS Images classification with uncertainty detection and image similarity

Davide Modolo (#229297)

Abstract
The proposed multi-stage model for predicting LUS image scores is built using three main components: a multi-class frame classifier, an uncertainty detection model, and a similarity module. The idea is to retrieve similar images and analyze them when the initial prediction is uncertain. The entire project is currently available on GitHub [1].

Introduction

This project aimed to develop an alternative way to predict LUS images scores. The first idea was to build something that could be useful as a tool helping with the final decision when the score of a specific frame was uncertain.

The existing methodology consists in scoring all 14 different spots and summing their values. If the result is $< 24/42$, the patient can be left going home because it indicates a low probability of worsening.

As explained in the article by S. Roy et al. [2], LUS images are scored as:

- 0: no artifact in the picture;
- 1: at least one vertical artifact (B-line);
- 2: small consolidation below the pleural surface;
- 3: wider hyperechogenic area ($< 50\%$) below the pleural surface.

Frames are from videos taken using ultrasound probes in a maximum of 14 different spots (6 on the front and 8 on the back of the patient), as explained in the article by G. Soldati et al. [3].

The proposed model consists of three main components:

- A multi-class frame classifier that predicts the score of individual LUS images;
- An uncertainty detection model that evaluates the confidence of the initial prediction;
- A similarity module that retrieves similar images and analyzes them when the first model is not confident.

With this multi-stage approach, the aim is to provide technicians with a different (hopefully reliable) diagnosis tool.

1. Data

We have been given a partial dataset from the San Matteo hospital, consisting of 11 patients for a total of $\sim$47k frames.

The dataset score distribution is shown in Figure 1a; at first glance, it could seem to be almost balanced (with only the score 1 that has fewer frames), but in reality, many patients are inherently unbalanced with some of them with the majority of frames only with a couple of scores (the score distribution for each patient is shown in Figure 2).
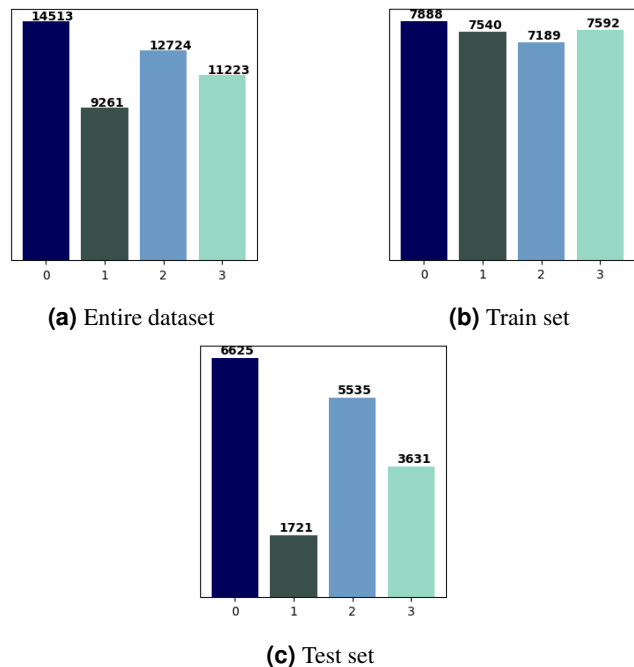

(a) Entire dataset

(b) Train set

(c) Test set

Figure 1. Score distribution in the dataset

1.1 Augmentation

Using the raw dataset resulted in overfitting even during the first epoch. To address this issue some transformations were implemented, taking a cue from the article [2].

In specific, each transformation is activated with a probability of 50%. The set of my augmentation function is:

- affine transformations (translation = $\pm15\%$, rotation = $\pm15°$, scaling $\pm45\%$, and shearing = $\pm4.5°$);
- multiplication with a constant ($\pm45\%$);
- Gaussian blurring ($\sigma = 3/4$);
- horizontal flipping ($p = 0.5$).

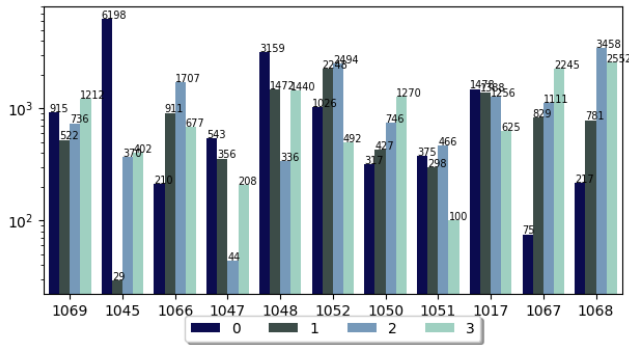**Figure 2.** Number of frames for each score for each patient (log scale for better visualization).

1.2 Data splitting

Having 11 patients available, the first approach involved 8 of them used to train the model and the remaining 3 for testing. This was due to the fact that using a portion of the frames for a patient in the test set and another in the training set easily leads to overfitting. Even dividing by exams would not be effective since different exams for the same patients still have a big correlation.

To choose the best configuration, the first attempt was to test with a *k-fold* approach and then choose the best fold, but having 165 combinations with $> 4h$ of computing time per combination required too much time resulting in an unfeasible process.

So, to balance the dataset, the standard deviation within scores for each 8-patient combination was computed and the one with the lowest std has been selected (red dot in Figure 3), resulting in the division shown in Figure 1b; the problem now was with the test set, that resulted to be very unbalanced (Figure 1c). After different attempts to balance both sets, I decided to just select an equal number of images for each score from the testing patients set of frames to use in the `test_model` method (still, confusion matrices on this report are built using the entire available test set).

2. Multi-class classifiers

The first module of this project consists in a deep learning classifier that predicts the score from a frame.

Different pre-trained models have been tested with several different values for the hyperparameters. The training part has been run several times in order to find a model that didn't overfit in the first epoch or didn't output only one single score.

In general, using models that are too big could lead to overfitting and using models that are too small could get no good generalization capability.

2.1 ResNet18

ResNet (Residual Network) is a network introduced by K. He et al. [4] trained on the ImageNet dataset [5].

There are different versions of this model based on the number of layers. Looking for a "small" model, ResNet18
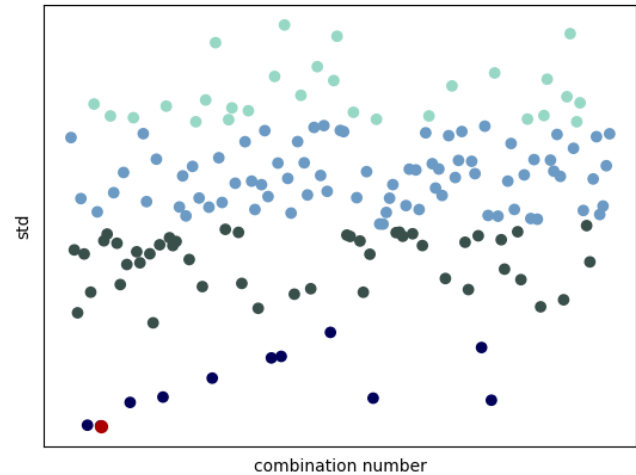

Figure 3. Standard deviation within the number of frames per score of every combination of 8 patients, the red one is the minimum (and so, it is the selected combination).

was the smallest one and so it has been selected for testing.

After many runs, the accuracy achieved was $\sim 56.65\%$ in the test set before overfitting. The confusion matrix on the test set can be seen in Figure 4, resulting in an accuracy class-wise that can be seen in Table 1, with a better generalization capability for classes 0 and 3 and a bit worse for classes 1 and 2.

0	1	2	3
55.53%	66.88%	40.43%	77.03%

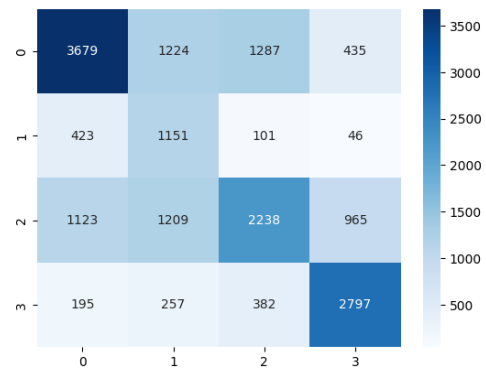**Table 1.** Accuracy class-wise of the fine-tuned ResNet18.

Figure 4. Confusion matrix of the fine-tuned ResNet18.

2.2 VGG16

VGG (Visual Geometry Group) is a convolutional Neural Network built by K. Simonyan, A. Zisserman [6]. It has been trained on a subset of the ImageNet dataset.

Similarly to ResNet, VGG is available with 16 and 18 layers. For the same reasons as above, VGG16 has been selected and tested.

Independently from the numerous fine-tuning tries, VGG16 started memorizing the training data in the first epoch (even if it has fewer parameters than ResNet18) so this approach has been immediately discarded.

2.3 SqueezeNet

SqueezeNet is a model developed by F. N. Iandola et al. [7] in 2016 trained on ImageNet.

Following the idea of finding a compact model, this variation of AlexNet is still capable of very good performance while requiring fewer parameters.

SqueezeNet gave me the best results in the early stage of the project, but after refining the fine-tuning of the ResNet, it was discarded.

2.4 Built-from-scratch model

A Convolutional Neural Network built from scratch has also been tested. It has been tried with several Convolutional layers down to only one, but the results were very poor, resulting in an approach that was not interesting for this project to follow deeper.

3. Binary classifiers

The second goal of this project was to develop a mechanism to determine the confidence of the multi-class frame classifier in its predictions.

Initially, the possibility of using a threshold-based approach was explored; however, during the in-class presentation, we realized that a more sophisticated approach would be interesting to try to capture the behaviour of the model in both correct and incorrect predictions. In addition, the maximum softmax values when the classifier was correct and when it was not were very similar, indicating that a simple threshold approach would not have been valid.

As a result, two binary classification models were developed; they use the softmax values of the first model to evaluate the confidence in its predictions.

To train these models, the data has been built by using the trained ResNet18 model on the training set to save the output values with their correctness (T/F); it was also required to balance the new dataset since a dataset that was even a bit unbalanced would lead to one and only one output value.
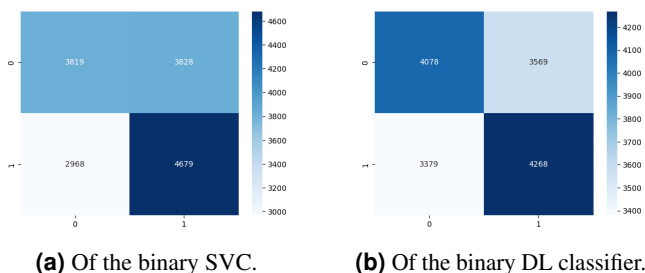
3.1 Deep model

For this approach, a simple neural network with four inputs and two outputs has been built. It uses one dense layer with a Sigmoid activation function to make predictions (ReLU has also been tested but resulted in worse performance).

Any added layer or complexity resulted in a very bad performance, but with this basic configuration, it was possible to achieve 54.66% accuracy in one of the many runs (with similar results in both classes, Figure 5b).

3.2 Support Vector Classifier

From the `sci-kit learn` library, SVC is a linear model that tries to find the best hyperplane that separates the two classes. The SVC model can be trained quickly and its performance was similar to the deep learning model created, but it was more prone to "overfitting" since even a dataset that was a little unbalanced in the class distribution resulted in 50% accuracy (so, random choice). The final SVC got 56.34% accuracy, built with a perfectly balanced dataset (with better performance in finding a correct prediction, Figure 5a).

3.3 Four SVCs

To investigate further the behaviour of the SVC, one different SVC for each class has been tested. The idea was: "Depending on the class predicted by the first classifier, one of the four SVCs will be called, trying to have a more specific approach".

The average accuracy by class is 54.2%, worse than the single SVC, but still good. The results seemed fine until the implementation in the final model where it got worse results than both the Deep Learning model and the single SVC (with an accuracy on the field of ∼36%).

4. Image similarity

The third module of the project consists of an image similarity model. As briefly said before, this idea was born from the definition of diagnosis that has some degree of subjectivity. Of course, thanks to the scoring mechanism proposed and cited in Introduction, this effect is mitigated. Still, the idea of showing similar images when the score prediction had low confidence can be interesting to explore.

Only a portion of the available images from the train set has been used since every approach has a working time too high with the entire dataset. The solution was to randomly pick the same number of images for each score for each patient from the training set (for a new total of 1408 frames, 352 of each score) and again in the test set (for a new total of 348 frames, 87 of each score) to compare every approach (but of course having this number of frames and patients, results are not very reliable).

4.1 Near Duplicate Image Search

Near Duplicate Image Search is a technique for finding similar images using a nearest neighbour algorithm. The `Annoy` python library is a fast and efficient approximate nearest neighbour search library that was used to implement this module.

(a) Of the binary SVC. **(b)** Of the binary DL classifier.
Figure 5. Confusion matrices of binary classifiers.

The process involves converting each image into a high-dimensional feature vector (in this case, the fine-tuned ResNet18 features were used). The feature vector is then indexed using the Annoy library, which allows for retrieval of the most similar images based on their Euclidean distance.

This approach has been discarded since its performance seemed good, getting a maximum accuracy of 59.06%, investigating the behaviour, almost 60% of the images haven't any nearest neighbour, so, even if the final model with this component has the highest numerical accuracy, it does not follow the idea of finding similar images when required. This issue could probably be resolved by increasing the number of images selected to build the feature vector, but this process would be very slow. In addition, for the images with available nearest neighbours, the only output score was 2.

4.2 t-SNE

t-SNE (t-Distributed Stochastic Neighbor Embedding) is a machine learning algorithm used for data visualization. It maps high-dimensional data points into a low-dimensional space, typically two or three dimensions while preserving the pairwise similarities between the points.

It's a technique used in computer vision to find images that are visually similar to a given query image. The goal is to identify images that are duplicates, or nearly identical, to the query image.

While both t-SNE and near duplicate image search are used in computer vision, they have different purposes and applications. t-SNE is used for visualizing high-dimensional data, while near duplicate image search is used specifically for identifying visually similar images.

So, while Near duplicate image search should fit better the scope of this project, t-SNE got better results overall.

4.2.1 Embeddings

Using the fine-tuned ResNet18, once again the embeddings from the training set were taken. Then, the t-SNE was built for each test image and the mean, minimum, maximum, mode, and median values were computed across the scores of 1 to 15 neighbours. The best result was 49.42% accuracy with *7 neighbours* and the function *minimum* (Figure 6).
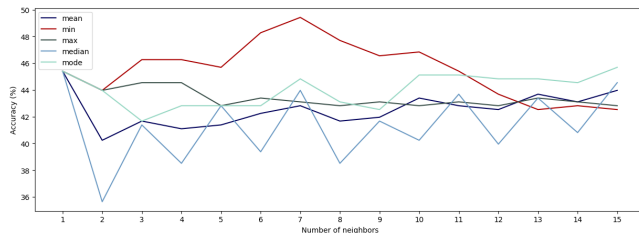

Figure 6. Comparison between neighbours in t-SNE using ResNet18 embeddings.

Embeddings with no t-SNE While working on the t-SNE based on embeddings, a test using the embeddings as they were was run, computing the cosine similarity to find the closest *n* images (Euclidian distance has also been tested but resulted in even worse results).

> "It is measured by the cosine of the angle between two vectors and determines whether two vectors are pointing in roughly the same direction" [8].

It got better results than Near Duplicate Image Search (since it was at least able to output different values) but worse than any t-SNE approach, with an accuracy on the entire test dataset of 38.46%.

This approach was tested and the best configuration was found by taking the *mode* of the scores across the *14 nearest* images.

4.2.2 Raw Images

Using flattened raw images to create a t-SNE was the worst approach.

As in every try, the mean, minimum, maximum, mode, and median values were computed across the scores of 1 to 15 neighbours.

In this case, results were not promising since the maximum accuracy was 26.72% with *2 neighbours* and the function *mean* (Figure 7).
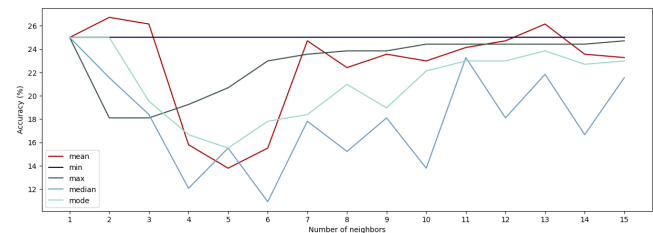

Figure 7. Comparison between neighbours in t-SNE using raw images as inputs.

4.2.3 Behavior

Last, a t-SNE using the softmax values of the first classifier was built. Even if this representation is not based on visually similar images, it got the best results across all the t-SNE approaches.

As before, the mean, minimum, maximum, mode, and median values were computed across the scores of 1 to 15 neighbours. The best accuracy was 54.88%, found with *11 neighbours* and the function *mode* (Figure 8).
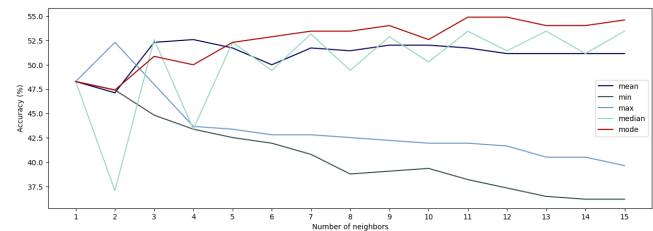

Figure 8. Comparison between neighbours in t-SNE using classifier softmax results as inputs.

5. Performance analysis

Regarding the final model, almost all possible configurations of the three components were tested. Although the behavior of each set of three modules was quite similar, the configuration that achieved the best accuracy was the one consisting of the three models that individually produced the best results.

The three components used in the final model are:

- ResNet18
- Single SVC
- t-SNE behaviour version

The same subset of images was used for testing all the components again. The result testing set is made of 348 images. The confusion matrices for this new test set of each module and the final model are in Figure 9, denoting a similar behaviour for every module of the final model.
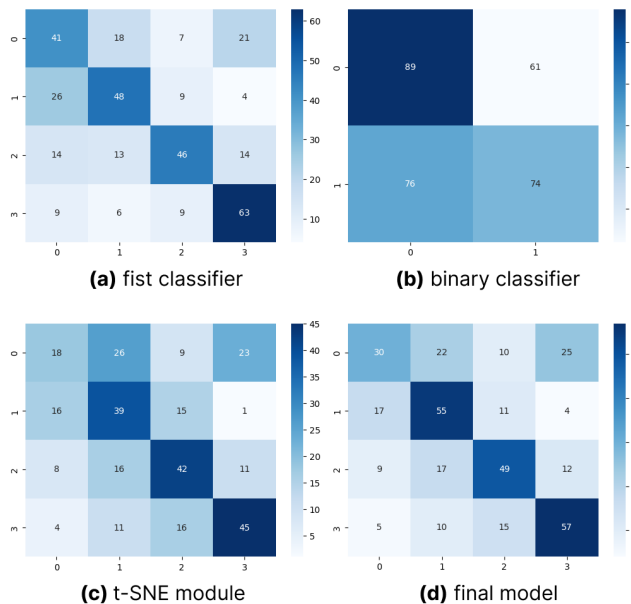

(a) fist classifier

(b) binary classifier

(c) t-SNE module

(d) final model

Figure 9. Confusion matrices

Unfortunately, the average accuracy of the final model on this new test set is very similar to the one of just the classification model. Starting from a 56.9% accuracy of the classifier, with the 54.33% of the binary and with 48% of the t-SNE module, the final model achieved a 54.89% accuracy in the end.

Having three components in the model means having three potential points of failure. In specific, the behaviour of the binary model in the final model was analyzed and it showed that, probably due to the little amount of data used to train it, it only got the right prediction on 3059/17512 images (the entire test set), getting almost always the correct result for the label 1, less than 25% of the time with label 2 and very few times with labels 0 and 3.

In addition to this, the similarity module uses only a small subset of the training images and it could be that most of the time the binary model states the first one is not a correct prediction it overlaps with the wrong results from the analysis of the similar images.

In general, there is not a single component that breaks the entire machine, as performances are similar across all the scores and all the modules.

6. Conclusions

Based on the analysis, the proposed model did not achieve the desired results. Despite testing multiple configurations and using various components, the final model's accuracy was slightly worse than the one of the classification model alone. Furthermore, one of the modules (the binary model) did not perform well, potentially due to the limited amount of data used to train it.

It is also possible that the similarity module's reliance on a small subset of training images could have led to incorrect predictions. While there isn't a single component responsible for the model's lack of success, it seems that having multiple potential points of failure could have contributed to the final performance.

Overall, it appears that the proposed model needs further improvements and adjustments to achieve better or more valuable results. However, it is important to note that the project was still valuable as it provided insights and learning experiences, but the effectiveness of the proposed model in practical applications is questionable.

6.1 Future works

Since this project is built with many components, several different things can be done to try to improve it:

- Test more pre-trained models: there are dozens of models out there that are capable of multi-class image classification, there could be one that works better with this specific project;

- Use more data: As the binary model's poor performance may have been due to limited data, collecting more data could help improve the binary model's accuracy;

- Locality Sensitive Hashing: it's a variant of the Near Duplicate Image Search methodology that uses a special hashing function to encode the images, but the implementation is not trivial;

- Speed up t-SNE using the CUDA version developed by Chan et al. [9], in order to use more images for each t-SNE build or test different configurations of this method.

References

[1] GitHub repository with the project. [Online]. Available: https://github.com/davidemodolo/Lung-Ultrasound-Image-Classifier

[2] S. Roy, W. Menapace, S. Oei, B. Luijten, E. Fini, C. Saltori, I. Huijben, N. Chennakeshava, F. Mento, A. Sentelli, E. Peschiera, R. Trevisan, G. Maschietto, E. Torri, R. Inchingolo, A. Smargiassi, G. Soldati, P. Rota, A. Passerini, R. J. G. van Sloun, E. Ricci, and L. Demi, "Deep learning for classification and localization of covid-19 markers in point-of-care lung ultrasound," *IEEE Transactions on Medical Imaging*, vol. 39, no. 8, pp. 2676–2687, 2020.

[3] G. Soldati, A. Smargiassi, R. Inchingolo, D. Buonsenso, T. Perrone, D. F. Briganti, S. Perlini, E. Torri, A. Mariani, E. E. Mossolani, F. Tursi, F. Mento, and L. Demi, "Proposal for International Standardization of the Use of Lung Ultrasound for Patients With COVID-19: A Simple, Quantitative, Reproducible Method," *J Ultrasound Med*, vol. 39, no. 7, pp. 1413–1419, Jul 2020.

[4] K. He, X. Zhang, S. Ren, and J. Sun, "Deep residual learning for image recognition," 2015.

[5] ImageNet site. [Online]. Available: https://www.image-net.org/

[6] K. Simonyan and A. Zisserman, "Very deep convolutional networks for large-scale image recognition," 2015.

[7] F. N. Iandola, S. Han, M. W. Moskewicz, K. Ashraf, W. J. Dally, and K. Keutzer, "Squeezenet: Alexnet-level accuracy with 50x fewer parameters and <0.5mb model size," 2016.

[8] Cosine Similarity. [Online]. Available: https://www.sciencedirect.com/topics/computer-science/cosine-similarity

[9] D. M. Chan, R. Rao, F. Huang, and J. F. Canny, "Gpu accelerated t-distributed stochastic neighbour embedding," *Journal of Parallel and Distributed Computing*, vol. 131, pp. 1–13, 2019.